ARTICLE

Sniffing Chronic Renal Failure in Rat Model by an Array of Random Networks of Single-Walled Carbon Nanotubes

Hossam Haick,[†,‡,*] Meggie Hakim,[†] Michael Patrascu,[†] Chen Levenberg,[†] Nisreen Shehada,[†] Farid Nakhoul,[§] and Zaid Abassi[∥,¶]

[†]Department of Chemical Engineering, Technion-Israel Institute of Technology, Haifa 32000, Israel, [‡]Russell Berrie Nanotechnology Institute, Technion-Israel Institute of Technology, Haifa 32000, Israel, [§]Ambulatory Nephrology Unit, Rambam-Health Care Campus, Haifa 31096, Israel, [∥]Faculty of Medicine, Technion-Israel Institute of Technology, Haifa 31096, Israel, and [¶]Research Unit, Rambam-Health Care Campus, Haifa 31096, Israel

ABSTRACT In this study, we use an experimental model of bilateral nephrectomy in rats to identify an advanced, yet simple nanoscale-based approach to discriminate between exhaled breath of healthy states and of chronic renal failure (CRF) states. Gas chromatography/mass spectroscopy (GC—MS) in conjugation with solid-phase microextraction (SPME) of healthy and CRF breath, collected directly from the trachea of the rats, identified 15 common volatile organic compounds (VOCs) in all samples of healthy and CRF states and 27 VOCs that appear in CRF but not in healthy states. Online breath analysis *via* an array of chemiresistive random network of single-walled carbon nanotubes (SWCNTs) coated with organic materials showed excellent discrimination between the various breath states. Stepwise discriminate analysis showed that enhanced discrimination capacity could be achieved by decreasing the humidity prior to their analysis with the sensors' array. Furthermore, the analysis showed the adequacy of using representative simulated VOCs to imitate the breath of healthy and CRF states and, therefore, to train the sensors' array the pertinent breath signatures. The excellent discrimination between the various breath states obtained in this study provides expectations for future capabilities for diagnosis, detection, and screening various stages of kidney disease, especially in the early stages of the disease, where it is possible to control blood pressure and protein intake to slow the progression.

KEYWORDS: renal failure · breath · detection · carbon nanotube · volatile biomarker

End-stage renal disease (ESRD) is a debilitating medical condition of chronic renal failure (CRF), which requires intensive and costly treatments through dialysis or transplantation. Treatment rates for ESRD have risen over the last 25 years in the western world.[1] This is due to increasing prevalence and incidence of ESRD in all high-income countries for several reasons, including the aging of the population, increasing diabetes rates, improved survival from heart disease, and wider acceptance to dialysis therapy. Health systems are grappling with how to allocate resources within their ESRD programs while balancing the competing objectives of cost containment and achieving good outcomes.[2]

The hitherto known methods for diagnosing renal failure include physical examination wherein symptoms such as oral ulcers and pallor may indicate kidney disorder among other diseases and disorders.[3] Blood tests and urinalysis are commonly used, wherein high levels of creatinine and blood urea nitrogen (BUN) are usually attributed to a decline in kidney filtration.[3,4] However, these tests tend to be highly inaccurate and may remain within the normal range even while 65—75% of kidney function is lost. Urinary kidney injury molecule-1 (KIM-1) is an important biomarker for the detection of (early stages of) kidney disease. Several sensing technologies have been proposed to target this (KIM-1) biomarker,[5—7] but KIM-1 antibody functionalized AlGaN/GaN high electron mobility transistors (HEMTs)[7] seem to have clear technological advantages. Imaging techniques are also applied to detect changes in size, texture, and position of the kidneys.[4] These measurements are performed using ultrasound and are suitable only in patients suffering from progressive renal failure. Presently, renal biopsy remains the most definitive test to specifically diagnose chronic and acute renal failure. This method is invasive and thus comprises the risk of infections and bleeding among other possible complications.[8] Accurate interpretation of the renal biopsy also demands the expertise of a pathologist with extensive experience in analyzing a biopsy sample for evidence of renal dysfunction.[4,8] Hence, there is an unmet need for a noninvasive method for detection of renal failure of various etiologies. Furthermore, the challenge remains to diagnose renal disorders with sufficient sensitivity and specificity to provide a large-scale screening technique, feasible for clinical

*Address correspondence to hhossam@technion.ac.il.

Received for review February 21, 2009 and accepted April 21, 2009.

Published online April 27, 2009.
10.1021/nn9001775 CCC: $40.75

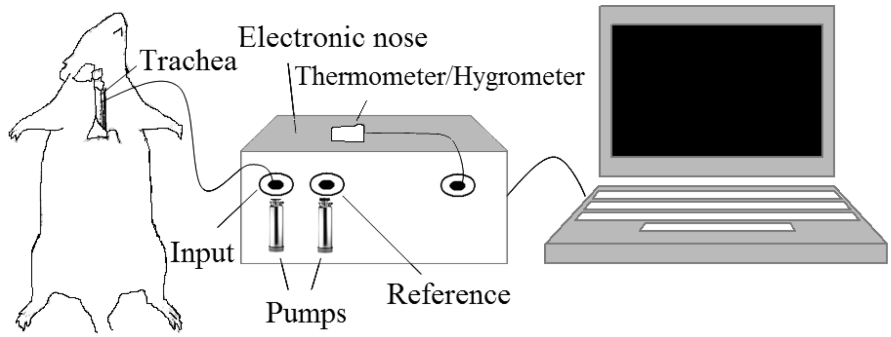

Figure 1. Schematic illustration of the experimental system used to collect breath normal rats and animals that underwent bilateral nephrectomy (see ref 17).

practice, for people at increased risk of developing renal dysfunction.

Using an array of quartz crystal microbalance (QCM) sensors in conjugation with pattern recognition methods, kidney disorders were detected by analyzing volatile biomarkers in the headspace of urine samples containing blood residues of kidney patients.[9] However, the analytes actually being detected by that system are currently unknown, and no information is available about whether this signature was independent of stage or was associated with the type of kidney disease. In another study, headspace of blood samples was analyzed using an array of 14 conducting polymer sensors and compared to traditional biochemistry tests.[10] Pattern recognition and hierarchical cluster analysis were applied to evaluate the data and demonstrated the ability to distinguish between predialysis blood from postdialysis blood. In certain instances, however, using blood has several disadvantages, such as (a) blood samplings are invasive; (b) blood contains complicated mixtures of compounds that could screen important volatile biomarkers of the disease; and (c) blood samples require time-consuming adaptations prior to their analysis (*e.g.*, agitation, incubation, *etc.*) to enhance the presence of volatile biomarkers in the headspace of blood.

In 1977, Simenhoffet *et al.* showed, using low-resolution electron-impact gas chromatography/mass spectroscopy (GC−MS), that dimethylamine and trimethylamine appear to be elevated in exhaled breath of ESRD instances, with subsequent reduction after hemodialysis.[11] On the basis of these observations, an array of QCM sensors coated with simulated olfactory receptor proteins was used to detect kidney diseases *via* breath samples.[12] In clinical tests, this module discriminated the normal subjects properly from patients but could not provide reliable discrimination between patients with uremia, chronic renal insufficiency, or chronic renal failure.[12] Furthermore, the collection process of breath samples in this study was uncontrolled and suboptimal. For instance, the exhaled breath of ESRD patients was collected directly from the mouth, where exogenic volatile metabolites of oral origin can contribute to the "uremic breath", thus interfering with the interpretation of the results. In addition, the speed of the expiration and other collection conditions that might affect the content of the volatile metabolites were not standardized.

In this study, we use an experimental model of bilateral nephrectomy in rats to identify advanced, yet simple nanoscale-based approach to discriminate between exhaled breath of healthy states and of chronic renal failure (CRF) states. A technology, in which a (semi-) conductive random network of single-walled carbon nanotubes (SWCNTs) and insulating nonpolymeric organic materials provides arrays of chemically sensitive resistive vapor detectors, forms the basis for our approach (see ref 13).[14−16] Using SWCNT networks circumvents the requirement of position and structural control (as is the case in devices based on individual SWCNT) because the devices display the averaged usual properties of many randomly distributed SWCNTs.[14−16] An additional feature of SWCNT networks is that they can be processed into devices of arbitrary size using conventional microfabrication technology. Using a rat model rather than human breath at this stage would allow better control over the experimental conditions and, subsequently, more reliable and valid results. For example, in the applied rat model, pure ESRD can be produced without any background metabolic or systemic diseases (*e.g.*, diabetes mellitus, hypertension, *etc.*) that may be responsible for the generation of volatile metabolites unrelated to kidney disease. In addition, this model of ESRD is fast and reaches its maximal severity within 48 h, allowing the accumulation of only renal-failure-related compounds (Figure 1). Moreover, in this animal model, the breath samples are collected directly from the trachea rather than the mouth, thus minimizing oral or nasal contaminations (see ref 17). Finally, bilateral nephrectomy in rats enables inducing consistent ESRD where all rats have zero renal function, as compared with human ESRD, where remnant renal function of variable extent still persists.

RESULTS AND DISCUSSION

Breath Analysis Using GC−MS. Classic chemical analysis of blood samples for creatinine and urea concentrations revealed that rats that underwent bilateral ne-

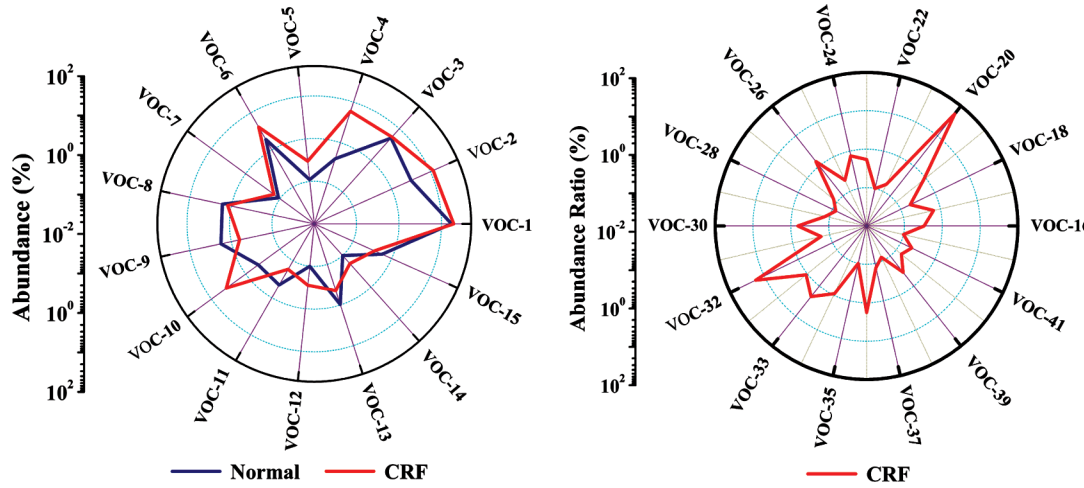

Figure 2. Abundance of (a) common VOCs appear in both healthy and CRF states, and (b) VOCs appear in CRF but not in healthy states. The abbreviation of each VOC is presented in Table 1.

phrectomy displayed remarkable elevation of creatinine (8.73 ± 0.73 *vs* 0.42 ± 049 mg%, $P < 0.001$) and BUN (218.0 ± 13.74 *vs* 19.8 ± 2.2 mg%, $p < 0.001$) as compared with sham controls. The obtained levels of both urea and creatinine in the nephrectomized rats are extremely high and corresponding to the values usually measured in clinical ESRD. It should be emphasized that, by using this radical experimental model, we produced explicit ESRD, where plasma levels of creatinine and urea reflect complete, convincing loss of kidney function. In contrast, using mild or moderate CRF at this stage of assessing the validity of our sensing approaches may yield marginal circulatory levels of these metabolites and give false negative and false positive results.

TABLE 1. Abbreviations of the Volatile Organic Compounds (VOCs) Detected by the GC−MS Analysis for Health and CRF Breath States[a]

VOC #	Chemical	VOC#	Chemical
1	phenol	23	ethyloxirane
2	decane	24	toluene
3	*N*,*N*-dimethyl acetamide	25	2-methyl-1-propene
4	3-ethylhexane	26	isopropyl palmitate
5	undecane	27	acetic acid
6	4-ethyl-5-methylnonane	28	2,3,3-trimethylpentane
7	2-bromoheptane	29	2-ethyl hexanol
8	2,4-dimethylheptane	30	2-propyl-1-heptanol
9	4-methyloctane	31	1,2-benzenedicarboxylic acid
10	2-methylundecane	32	trimethylamine
11	3,5-dimethyloctane	33	6-nitro-2-picoline
12	5,7-dimethylundecane	34	6-undecylamine
13	propane	35	phenethylbenzonitrile
14	3-methyl-4-nonene	36	2*H*-pyran
15	oxalic acid	37	*N*-morpholinomethylisopropylsulfide
16	ethanol	38	*N*-dimethylaminomethyl
17	acetic acid	39	9-decyl-9-borabicyclononane
18	isopropyl alcohol	40	2-phenylacenaphthenopyrrole
19	acetone	41	cyclobutane
20	dimethylamine	42	sclareoloxide
21	dibutyl phthalate		
22	diphenyl ether		

[a]The abundance of the listed VOCs is shown in Figure 2.

Compared with the previous low-resolution GC−MS experiments, which identified limited (2−4) VOCs,[11] the current GC−MS analysis of breath samples identified 100−180 different VOCs that had been either synthesized or catabolized in at least one healthy state or in one CRF state. However, forward stepwise discriminant analysis identified 15 common VOCs that appear in all samples of healthy and CRF states, with >90% confidence. As shown Figure 2a and Table 1, the common compounds are mostly phenol, oxalic acid, and derivatives of C_3-C_{11} alkanes. Excluding 4-methyloctane (VOC-9), 3,5-dimethyloctane (VOC-11), and propane (VOC-13), all other VOCs appear to be elevated in instances of CRF, as compared to healthy states. Further forward stepwise discriminant analysis revealed 27 VOCs that appear in CRF states but not in healthy states (Figure 2b). Generally speaking, these compounds could be classified into derivatives of amines, alkenes, acids, and alcohols. Among all of these 27 VOCs, dimethylamine (VOC-20) and trimethylamine (VOC-32) exhibited the highest concentration levels. The observation of 42 CRF VOCs in our study, rather than 2−4 VOCs as reported earlier,[11] could be attributed to the effect of SPME fibers on the VOCs extraction (in general, polar fibers are used for polar analytes and nonpolar types for nonpolar analytes).[18,19] For example, PDMS fiber extracts *via* absorption with analytes dissolving and diffusing into the bulk of the coating. The remaining types (PDMS/DVB and PDMS/carboxen) are mixed coatings and extract *via* adsorption of analytes staying on the fiber's surface, which, for the most part, could be ascribed to highly volatile solvents and gases. Furthermore, the GC−MS detector used in the current study has detection capabilities and resolution significantly higher than that reported previously.[11]

The saturated hydrocarbons (*e.g.*, C_3-C_{11}) obtained in the breath of studied samples can reasonably be at-

tributed to lipid peroxidation of fatty acid components of cell membranes, triggered by reactive oxygen species.[20−22] *In vitro* studies have shown that the evolution of hydrocarbon as the end products of polyunsaturated fatty acids correlates very well with other markers of lipid preoxidation.[20] Although there are other sources of hydrocarbons in the body, such as protein oxidation and colonic bacterial metabolism,[20] these apparently are of limited importance and do not interfere with the interpretation of the hydrocarbon breath test because they appear in smaller quantities. They have a low solubility in the blood and hence are excreted in the breath within minutes of their formation. Propane (VOC-13) is mainly derived from protein oxidation and fecal flora, and their role as markers of lipid peroxidation is doubtful. Methylated hydrocarbons have also been described as lipid peroxidation markers.[23,24] However, the biochemical pathways of generation and the physiological meaning of these compounds have not yet been elucidated in sufficient depth.[25]

Oxygen-containing compounds such as ethanol (VOC-16) and acetone (VOC-19) were found in the breath of CRF states only. The detection of the ethanol content of exhaled breath is not directly connected to a disease.[26] Still, the potential source of endogenous ethanol is the intestinal bacterial flora.[27] As for acetaldehyde, concentrations of ethanol in humans are always lower than acetone, which produced by decarboxylation of acetoacetate which is derived from lipolysis or lipid peroxidation.[28] Usually, breath acetone concentrations are increased in patients with (uncontrolled) diabetes mellitus.[29] However, in our case, it is more likely that acetone emerges from fasting, starvation, or hepatic disturbance concomitant with renal disease.[30,31]

The *N*-morpholinomethylisopropylsulfide (VOC-37), which was observed in CRF states only, can be generated by incomplete metabolism of methionine in the transamination pathway.[32] Under normal conditions, concentrations of sulfur-containing compounds in human blood and breath are very low. Impairment of liver function increases the level of sulfur-containing compounds.[33,34] Simple nitrogen-containing solutes that accumulate in uremia include the aliphatic amines, monomethylamine, dimethylamine, and trimethylamine. These compounds are produced by both gut bacteria and mammalian cells. They are positively charged at physiologic pH, and their removal during intermittent hemodialysis may be limited by their preferential distribution within the relatively acidic intracellular compartment.[35] The existence of these compounds exclusively in breath of CRF rats indicates that these compounds emit from blood to breath. The phenol (VOC-1) amounts detected in breath can be derived from the amino acids tyrosine and phenylalanine and from aromatic compounds, similar to the way aromatic rings exist in uremic solutes.[36] In this context, it should be mentioned that significant correlations between urinary phenols (*p*-cresol, phenol) and certain groups of mucosal flora (staphylococci, bacteroides) of the small intestine of normal rats has been reported.[37] In this case, metabolism of parent compounds by methylation, dehydroxylation, oxidation, reduction, or conjugation produces a bewildering array of solutes. The structural similarity of waste phenols to neurotransmitters has encouraged speculation that these compounds interfere with the function of the central nervous system, but evidence of the toxicity of individual compounds is weak.[38] The origin of the other VOCs is not known. Additional investigations are needed to learn about the important biochemical pathways for all of the volatiles that can be detected.[22]

Despite the progress that has been achieved with GC−MS, this method has not been accepted as an accredited diagnostic tool. Apart from the cost of the equipment, the main reason is the complexity of its use. Because of the measurement time and the need for qualified labor in its operation, it is not used either in diagnosis or for health monitoring. Therefore, the introduction of an easy-to-use diagnostic device, based on an array of sensors, would open up new fields of application.

Sniffing CRF by SWCNT Sensors. In contrast to the "lock-and-key"-based devices,[39,40] wherein each sensor produces an electronic response from a single analyte, in the sensors' array approach, each sensor is widely responsive to a variety of odorants.[41,42] In this architecture, each analyte produces a distinct signature from the array of broadly cross-reactive sensors (a widely used terminology of this architecture can be electronic nose).[41,42] This configuration allows considerably widening the variety of compounds to which a given matrix is sensitive, increasing the degree of component identification and, in specific cases, performing an analysis of individual components in complex multicomponent mixtures. Pattern recognition algorithms can then be applied to the entire set of signals, obtained simultaneously from all the sensors in the array, in order to glean information on the identity, properties, and concentration of the vapor exposed to the sensor array.

In this study, an array of SWCNT sensors was used to distinguish between the overall breath pattern of healthy and CRF states, and the corrected sensor signals were analyzed using principal component analysis (PCA).[43,44] PCA is an effective method to reduce our multidimensional data space (10 sensors) to its main components and therefore improves the human perception ability of the data. PCA determines the linear combinations of the sensor values such that the maximum variance between all data points can be obtained in mutually orthogonal dimensions. This results in the largest variance between sensor values from the first principal component and produces decreasing magni-

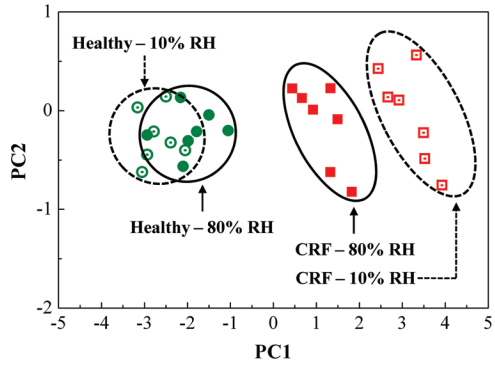

Figure 3. Principal component analysis plot of $\Delta R/R_b$ response of 10 sensors upon exposure to breath of healthy and CRF rats (with ~80% RH), before and after passing the breath in the dehumidifier that preceded introduction to the sensors' array.

tudes of variance from the second to the third principle components and so on.

The first and second principal components for each subject accounted for >92% variance and are drawn in Figure 3. The cluster of healthy controls that contained ~80% RH (green, filled circular points, surrounded by solid circle) was separated from all CRF breath at the same level of RH (red, filled square points, surrounded by solid oval) by 100% success. No overlapping area was obtained between the PCA of these categories. From Figure 3, it is obvious that principle components differ between breath at ~80% RH and breath at 10% RH. Furthermore, it is obvious that the lower the humidity, which was achieved by using a dehumidifier before the sensors' array, the better the discrimination between the healthy and CRF breath states. The overlapping area between the healthy breath at ~80 and ~10% RH indicates that the effect of humidity on healthy breath is relatively small. In contrast, no overlapping area was observed between the PCA clusters at ~80 and ~10% RH in the CRF breath, indicating the significant effect of the humidity in the analysis of the CRF states. The different effect of the humidity of the samples studied is expressed also in the cluster distribution. As observed in Figure 3, the cluster distribution of healthy states remained almost the same at low and high RH values. In contrast, the cluster distribution of the CRF states increased slightly after lowering the humidity level of the measured samples. Overall, in comparison with a previous study that targeted the discrimination between healthy and lung cancer states *via* breath samples,[15] the effect of the humidity on the discrimination between healthy and CRF states in the current study was less critical. This could be attributed to the VOCs in lung cancer states appear at concentration levels that are 50−120-fold lower than that of the CRF states.

Clinical trials for validating the efficiency of an array of sensors in diagnosing CRF or other kidney-related disease in a subject include the following aspects: (a) providing a system comprising a plurality of chemically sensitive sensors and a processing unit comprising pattern recognition algorithms wherein said pattern recognition algorithms receive sensor signal outputs from the electronic device and compares them to stored data; (b) exposing the sensor array of said electronic device to an actual breath of a subject; and (c) using pattern recognition algorithms to detect VOCs in the sample indicative of a kidney-related disease in the subject. While clinical studies are a straightforward approach for validating the efficiency of the sensors' array for CRF detection, these studies are time-consuming and expensive, so simpler approaches are called for. A promising way to achieve this objective detection is by using "artificial" mixtures of VOCs that simulate the CRF and healthy states, based on the GC−MS observation for the same cases studied.[15,16] This approach provides three main advantages over the clinical studies during the development and/or adaptation of an array of sensors because it can determine precisely[15,16] (I) the signature of each individual CRF volatile biomarker on the developed array; (II) the correlation between the sensor's sensitivity and specificity of the individual VOC biomarkers to its existence in a pattern (or mixture) of other compounds; and (III) the necessary iterative feedback on sensors viability without the intervention of (disruptive) parameters—for example, patients' diet, metabolic state, genetics, *etc.*

With this in mind, representative VOCs that were detected in most CRF samples at the highest concentration levels were simulated *via* a homemade system and exposed to the sensors' array. The VOCs phenol, 2-ethyl hexanol, acetic acid, and undecane were chosen. In addition to these representative VOCs, water was used to simulate the saturated humidity in the exhaled breath. The response ($\Delta R/R_b$, where R_b is the baseline resistance of the sensor in the absence of analyte, and ΔR is the baseline-corrected steady-state resistance change upon exposure of the sensor to analyte) of the sensors' array to the different CRF VOCs at concentrations between 0.5 and 100 ppm was first examined. The sensors' responses were rapid upon exposure to vapor analyte, fully reversible upon switching back to zero vapor analyte (purified, dry air), responsive to a wide variety of concentrations, and showed a satisfying signal-to-noise ratio (not shown). Representative response patterns for the chosen VOC biomarkers at a given P/P^0 (=0.05) are shown in Figure 4. As observed in the figure, each of the developed sensors is broadly responsive to a variety of biomarkers and each biomarker produces a distinct fingerprint from the array of broadly cross-reactive sensors. In general, sorption of biomarkers showed change in resistance with exposure to an analyte, due to one or more of the following mechanisms: (I) charge transfer from adsorbed species to the carbon nanotubes;[45] (II) modifications of contact work functions;[46] and (III) carrier scattering by adsorbed species.[16,47]

On the basis of the GC−MS analysis of real breath samples (Figure 2), we prepared simulated healthy and CRF breath patterns. The simulated breath patterns were prepared in 80 ± 1% RH background to simulate the background water vapor content in real human breath. As a simulated CRF breath, we took a mixture of 886 ± 31.9 ppb phenol (VOC-1), 58.4 ± 4.4 ppb undecane (VOC-5), 32.2 ± 4.6 ppb acetic acid (VOC-27), and 8.4 ± 1.8 ppb 2-ethyl hexanol (VOC-29) with 80 ± 1% RH, 16 ± 1% O_2, 77−79 ± 1% N_2, 5 ± 1% CO_2, and 1.0 ± 0.2 ppm CO. As a simulated healthy state, we took 549.9 ± 24.3 ppb phenol (VOC-1) and 6.3 ± 1.2 ppb 3-ethyl hexane (VOC-4) with 80 ± 1% RH, 16 ± 1% O_2, 77−79 ± 1% N_2, 5 ± 1% CO_2, and 1.0 ± 0.2 ppm CO.[48] Multiple exposures to each mixture were carried out, and data were obtained for the array of sensors. As observed in Figure 5a, the cluster of simulated healthy controls was separated from all simulated CRF breath by 100% success; no overlapping areas were obtained between the PCA of these categories. Preparing the same VOC mixtures in 10 ± 1% RH background resulted in better separation (or discrimination) between the healthy and CRF clusters (Figure 5b).

The overlapping area between the clusters of simulated and real breath samples indicates that the simulation approach is quite robust for purposes of "training" the sensors' array. The higher distribution of the simulated clusters, compared with the real ones, could be attributed to the low number (4 VOCs for simulating CRF states and 2 VOCs for simulating healthy states) of compounds used to produce the required mixtures, compared to those detected in the real breath (15 VOCs in healthy breath and 42 VOCs in CRF breath). Complementary to this argument, it is obvious that principle components also differ between ~80 and 10% RH and that the lower the humidity (*i.e.*, 10% RH vs 80% RH) the better the discrimination. Indeed, the cluster distribution at 10% RH was significantly lower than that at 80% RH. This observation could be attributed to the screening effect of the water molecules. At 80% RH, the water molecules appear at equivalent concentration level to the targeted VOCs. The different interaction and/or absorption of the water molecules with the different organic films of the sensing composites, however, causes different signals from the various sensors. In contrast to these observations, at 10% RH, the concentration of water is lower than targeted VOCs and, therefore, the effect of the latter is (more) perceivable.

SUMMARY AND CONCLUSIONS

In this study, we used an experimental model of bilateral nephrectomy in rats to identify advanced, yet simple approaches to discriminate between exhaled breath of healthy states and of CRF states. Using rat model rather than human breath allows better control of the experimental conditions and subsequently yields more reliable and valid results. GC−MS/SPME analysis

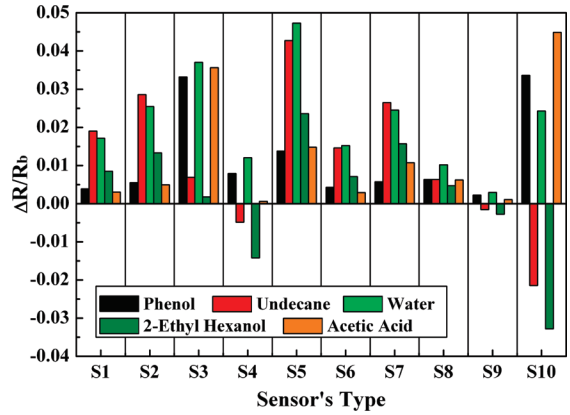

Figure 4. Response patterns for the representative CRF VOCs at $P/P^0 = 0.05$

of healthy and CRF breath, collected directly from the trachea of the rats, identified 15 common VOCs that appear in all samples of healthy and CRF states and 27 VOCs that appear in CRF states but not in healthy states. An important implication of these findings, besides the detection of diseases directly related to the respiratory tract, is the fact that VOCs are mainly blood borne and the concentration of biologically relevant substances in exhaled breath closely reflects that in the arterial system. Therefore, breath is predestined for monitoring different processes in the body.[49] Apart from the odor impression of CRF, much about the biochemical processes and the formation of marker substances is already known.[22] Analysis of the various breath

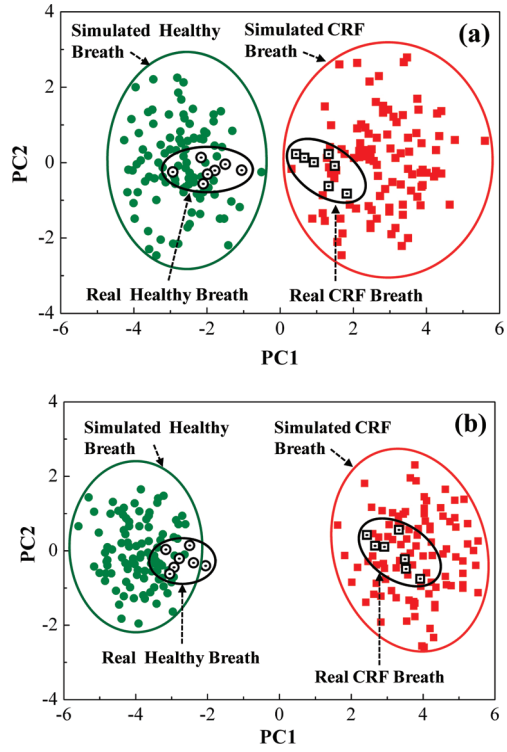

Figure 5. Real and simulated healthy and CRF patterns with (a) 80% RH and (b) 10% RH. Note: all data (real and simulated breath, at both given humidities) were run through PCA at the same time.

samples by an array of chemiresistive random network of SWCNTs showed excellent discrimination between the various breath states, while revealing significantly enhanced discriminations at lower humidity levels in the breath. Furthermore, we show that it is enough to use selected number of simulated VOCs to "train" the sensors' array system to discriminate between the electronic patterns of healthy states and CRF states. Experiments to distinguish less severe kidney failure (*e.g.*, 35−70% reduction in kidney function) and to distinguish CRF from other disease (or patho-physiological) states that have a potential to produce a distorted profile of breath VOCs (*e.g.*, liver failure, systemic infection, pneumonia, heart failure, *etc.*) are underway and will be published elsewhere.

Diagnosing CRF *via* breath samples has the potential for a noninvasive and easily repeatable test that is not disagreeable or embarrassing for the patient compared to blood or urine tests. In spite of the ease of the sampling procedure, special care should be taken to carry out the measurements in a reproducible way with human breath. Monitoring the nitric oxide (NO),[50] carbon monoxide (CO),[50] and ammonia (NH_3)[51] levels simultaneously during the measurements by, for example, electrochemical sensors, could contribute further to the accuracy of these measurements. The results presented in this study raise expectations for future capabilities for diagnosis, detection, and screening various stages of the kidney disease. Given the impact of rising incidence of kidney disease on health budgets worldwide, the proposed technology will be a significant saving for both private and public health expenditures.

MATERIALS AND METHODS

Animals. Studies were conducted on male Sprague−Dawley rats (Harlan Laboratories Ltd., Jerusalem, Israel), weighing 290−330 g. The animals were kept in a temperature-controlled room and fed standard rat chow containing 0.5% NaCl and tap water *ad libitum*. All experiments were performed according to the guidelines of the Technion's committee for supervision of animal experiments (Haifa, Israel).

Induction of ESRD. To resemble the clinical ESRD characterized by complete loss of kidney function, bilateral nephrectomy was performed. For this purpose, the animals were anesthetized with intraperitoneal injection of (a combination of) Nembutal (40 mg/kg) and placed on a temperature-regulated table (37 °C) to maintain the body temperature. For bilateral nephrectomy, the left and right renal arteries were exposed through a midabdominal incision and ligated with silk suture (4-0, Ethicon Ltd.) and both kidneys were removed. Sham operated rats served as controls. Following the surgical procedure, the animals were allowed to recover and then returned to their cages.

Blood Collection for Biochemical Analysis. Blood samples were collected either from rats with ESRD or healthy animals *via* the carotid arteries. Blood specimens were collected into tubes for determination of urea and creatinine levels by the classic colorimetric method (Rambam Biochemical Laboratories, Haifa, Israel).

Collecting Breath from Healthy and Operated Rats. Forty-eight hours after operation, sham rats or animals with bilateralnephrectomy (ESRD) were anesthetized by intraperitoneal injection of a combination of Nembutal (40 mg/kg; ip), placed on a temperature-regulated table (37 °C) to maintain the body temperature, and tracheostomy was performed for breath sampling within 2 h. The carotid artery was annulated for blood collection for measurement of urea, creatinine, and other waste products by classic methods.

For collecting breath samples, the trachea of rats was connected to a tube that split into inlet and outlet tubes, each connected to a one-way valve (Figure 1).[17] The outlet tube connected the rat to the sensors' array for breath analysis while the inlet tube enabled the rat to inhale air from the room. The experiments using sensor's array were done online, meaning that the rats breathed directly into the device and the diagnosis was achieved in real-time. In parallel to these experiments, 100−500 cm^3 breath samples were collected in Tedlar bags for off-line GC−MS analysis. Breath samples were collected from seven healthy rats and seven rats that had undergone the operation, during a period extending 6 months.

Analysis of Breath with GC−MS. The collected breath samples from healthy and operated rats were analyzed by GC−MS combined with solid-phase microextraction (SPME).[18,19,52] For our applications in breath tests, SPME can be thought of as a fiber coated with a solid phase that extracts different kinds of analytes from the gas phase.[18,19] The quantity of analyte extracted by the fiber is proportional to its concentration in the sample as equilibrium is reached after a relatively long time or, as pre-equilibrium is reached, after a relatively short time with help of convection or agitation. After extraction, the SPME fiber is transferred to the injection port of GC−MS, where desorption of the analyte takes place and analysis is carried out. The attraction of SPME is that the detection limits can reach parts per trillion (ppt) levels for certain compounds, while GC−MS *per se* can reach a detection limit of part per million (ppm) only.

A manual SPME holder with an extraction fiber of 100 μm polydimethylsiloxane (PDMS), 65 μm polydimethylsiloxane/divinylbenzene (PDMS/DVB), and 75 μm polydimethylsiloxane/carboxen (PDMS/carboxen) (all purchased from Sigma-Aldrich) was inserted into the Tedlar bag containing breath samples. Between 100 and 500 cm^3 of breath sample was concentrated *via* SPME method for 2 h, after which the SPME was inserted into the injector of GC−MS, which worked using the splitless model. The oven temperature profile was 60 °C, 2 min. A capillary column HP-5MS 5% phenyl methyl siloxane (30 m length, 250 μm diameter, 0.25 μm thickness) was used. The column pressure was set to 8.22 psi, and the initial flow was 1 mL/min. The VOCs were determined using automated mass spectral deconvolution and identification system (AMDIS) software which was developed for spectral extraction and compound identification by GC−MS. Eventually, the molecular structures of the VOCs were determined *via* the standard modular set.

Sniffing Real Breath Using an Array of SWCNT Sensors. Exhaled breath samples were analyzed by an array of 10 chemiresistive random network of single-walled carbon nanotubes (SWCNTs) coated with organic materials, in conjugation with pattern recognition methods, as described elsewhere.[14−16] The sampling system delivers ambient air and the sample vapor to the sensors in sequence. Each sensor of the array undergoes a reversible change in electrical resistance when exposed to a vapor or analyte. Furthermore, resistance change of each sensor is unique because of chemical diversity of the sensor materials. Consequently, a pattern of resistance changes is obtained from the sensor array to a given vapor. Five analyses, at minimum, were performed on the exhaled breath of each sample.

Sniffing Simulated Breath with an Array of SWCNT Sensors. A computer-controlled automated flow system delivered pulses of representative biomarker(s) of VOCs, which were determined earlier by GC−MS analysis, at a controlled fraction of the biomarker(s) vapor pressure(s) to the detectors.[15] Oil-free air, obtained from a compressed air source, was used as a carrying gas for the VOC biomarkers. In a typical experiment, signals of sensor ar-

ray elements were collected for 2 min of clean air, followed by 3 min of analyte vapor in air, and then followed by another 2 min of clean air to purge the system. Data analysis of the signals that were collected from all the sensors in the array was performed using standard principal component and cluster analysis.

Acknowledgment. The research was funded by the Marie Curie Excellence Grant of the European Commission's FP6 and the Technion's Russell Berrie Nanotechnology Institute. The authors acknowledge Dr. Gang Peng and Dr. Ulrike Tisch (Technion, Haifa) for assistance and fruitful discussions, and Dr. Ayelet Fishman (Technion, Israel) for allowing access to her GC−MS. H.H. holds the Horev Chair for Leaders in Science and Technology.

REFERENCES AND NOTES

1. Dor, A.; Pauly, M.; Eichleay, M.; Held, P. End-Stage Renal Disease and Economic Incentives: The International Study of Health Care Organization and Financing (ISHCOF). *Int. J. Health Care Finance Econ.* **2007**, *7*, 73–111.
2. Vassalotti, J. A.; Stevens, L. A.; Levey, A. S. Testing for Chronic Kidney Disease: A Position Statement from the National Kidney Foundation. *Am. J. Kid. Dis.* **2007**, *50*, 169–180.
3. Schrier, R. W.; Wang, W.; Poole, B.; Mitra, A. Acute Renal Failure: Definitions, Diagnosis, Pathogenesis, and Therapy. *J. Clin. Invest.* **2004**, *114*, 5–14.
4. Meyer, T. W.; Hostetter, T. H. Medical Progress: Uremia. *N. Engl. J. Med.* **2007**, *357*, 1316–1325.
5. Vaidya, V. S.; Ramirez, V.; Ichimura, T.; Bobadilla, N. A.; Bonventre, J. V. Urinary Kidney Injury Molecule-1: A Sensitive Quantitative Biomarker for Early Detection of Kidney Tubular Injury. *Am. J. Physiol. Renal. Physiol.* **2006**, *290*, F517–F529.
6. Lequin, R. M. Enzyme Immunoassay (EIA)/Enzyme-Linked Imunosorbent Assay (ELISA). *Clin. Chem.* **2005**, *51*, 2415–2418.
7. Wang, H. T.; Kang, B. S.; Ren, F.; Pearton, S. J.; Johnson, J. W.; Rajagopal, P.; Roberts, J. C.; Piner, E. L.; Linthicum, K. J. Electrical Detection of Kidney Injury Molecule-1 with AlGaN/GaN High Electron Mobility Transistors. *Appl. Phys. Lett.* **2007**, *91*, 222101/1–222101/3.
8. Cross, J.; Jayne, D. Diagnosis and Treatment of Kidney Disease. *Best Prac. Res. Clin. Rheumatol.* **2005**, *19*, 785–798.
9. Di Natale, C.; Mantini, A.; Macagnano, A.; Antuzzi, D.; Paolesse, R.; D'Amico, A. Electronic Nose Analysis of Urine Samples Containing Blood. *Physiol. Meas.* **1999**, *20*, 377–384.
10. Fend, R.; Bessant, C.; Williams, A. J.; Woodman, A. C. Monitoring Haemodialysis Using Electronic Nose and Chemometrics. *Biosens. Bioelect.* **2004**, *19*, 1581–1590.
11. Simenhoff, M. L.; Burke, J. F.; Saukkonen, J. J.; Ordinario, A. T.; Doty, R. Biochemical Profile or Uremic Breath. *New Engl. J. Med.* **1977**, *297*, 132–135.
12. Lin, Y.-J.; Guo, H.-R.; Chang, Y.-H.; Kao, M.-T.; Wang, H.-H.; Hong, R.-I. Application of the Electronic Nose for Uremia Diagnosis. *Sens. Actuators, B* **2001**, *B76*, 177–180.
13. The development of this array of sensors, instead of utilizing current technology, is mainly prompted by the need for sensors that can provide simultaneously high sensitivity (down to ppb level of concentrations), stability, low costs, and fast responses. Following are a few examples of sensors that are of great interest but cannot be used properly for our applications: (I) state-of-the-art nanomechanical oscillators have high detection limits (down to sub-ppb levels), but the high costs of fabrication and high vacuum and low temperatures required for operation make them currently impracticable to some extent; (II) chemiresistors of conducting polymers are simple to implement but high response to humidity (also, when the humidity coexist in mixtures containing 1−10s ppm of nonpolar VOCs) can be a disadvantage; (III) chemicapacitors are more stable than chemiresistors but can take long times to respond and recover;[34] and (IV) polymer-coated surface acoustic wave (SAW) or quartz crystal microbalance (QCM)[15] sensors are relatively expensive and, mostly, limited to a detection level of few ppm.
14. Haick, H.; Peng, G. Carbon Nanotube Structures in Sensor Devices for Analyzing Biomarkers in Breath Samples; U.S. Prov. No. 61/056,841, **2008**.
15. Peng, G.; Trock, E.; Haick, H. Detecting Simulated Patterns of Lung Cancer Biomarkers by Random Network of Single-Walled Carbon Nanotubes Coated with Nonpolymeric Organic Materials. *Nano Lett.* **2008**, *8*, 3631–3635.
16. Peng, G.; Tisch, U.; Haick, H. Detection of Nonpolar Molecules by Means of Carrier Scattering in Random Networks of Carbon Nanotubes: Toward Diagnosis of Diseases *via* Breath Samples. *Nano Lett.* **2009**, *9*, 1362–1368.
17. Breath contains an intraoral part (the first to be exhaled) and an alveolar part (the last to be exhaled), with the latter being more closely representative of the volatile biomarkers present in the blood circulation. Collection of alveolar breath from human could be carried out non-invasively *via* specifically designed breath collection kit, as described earlier by Peng *et al.* in *Nano Lett.* 2008, 3631−3635. In contrast, non-invasive collection of alveolar breath from rats is inhibited by their low rate of exhaled breath. To overcome this deficiency, breath was collected directly from the rat's trachea. While this mode of breath collection is considered invasive, one should remember that the rats are served only as a study model and that the ultimate (or future) goal of this study is to detect CRF in human, where non-invasive breath collection is easily applicable.
18. Mills, G. A.; Walker, V. Headspace Solid-Phase Microextraction Procedures for Gas Chromatographic Analysis of Biological Fluids and Materials. *J. Chromatogr. A* **2000**, *902*, 267–287.
19. Amorimb, L. C. A.; Cardeal, Z. L. Breath Air Analysis and Its Use As a Biomarker in Biological Monitoring of Occupational and Environmental Exposure to Chemical Agents. *J. Chromatogr. B* **2007**, *853*, 1–9.
20. Kneepkens, C. M. F.; Lepage, G.; Roy, C. C. The Potential of the Hydrocarbon Breath Test As a Measure of Lipid Peroxidation. *Free Radical Biol. Med.* **1994**, *17*, 127–160.
21. Buszewski, B.; Kesy, M.; Ligor, T.; Amann, A. Human Exhaled Air Analytics: Biomarkers of Diseases. *Biomed. Chromatogr.* **2007**, *21*, 553–566.
22. Miekisch, W.; Schubert, J. K.; Noeldge-Schomburg, G. F. E. Diagnostic Potential of Breath Analysis—Focus on Volatile Organic Compounds. *Clin. Chim. Acta* **2004**, *347*, 25–39.
23. Phillips, M.; Cataneo, R. N.; Greenberg, J.; Grodman, R.; Gunawardena, R.; Naidu, A. Effect of Oxygen on Breath Markers of Oxidative Stress. *Eur. Respir. J.* **2003**, *21*, 48–51.
24. Phillips, M.; Cataneo, R. N.; Greenberg, J.; Gunawardena, R.; Rahbari-Oskoui, F. I. Increased Oxidative Stress in Younger As Well As in Older Humans. *Clin. Chim. Acta* **2003**, *328*, 83–86.
25. Mitsui, T.; Kondo, T. Inadequacy of Theoretical Basis of Breath Methylated Alkane Contour for Assessing Oxidative Stress. *Clin. Chim. Acta* **2003**, *333*, 93–94.
26. Paulsson, N. J. P.; Winquist, F. Analysis of Breath Alcohol with a Multisensor Arrayi. Instrumental Setup, Characterization, And Evaluation. *Forensic Sci. Int.* **1999**, *105*, 95–114.
27. Cope, K.; Risby, T.; Diehl, A. M. Increased Gastrointestinal Ethanol Production in Obese Mice: Implications for Fatty Liver Disease Pathogenesis. *Gastroenterology* **2000**, *119*, 1340–1347.
28. Davis, P. L.; Dal, C. L. A.; Maturo, J. Endogenous Isopropanolforensic and Biochemical Implications. *J. Anal. Toxicol.* **1984**, *8*, 209–212.
29. Lebovitz, H. E. Diabetic Ketoacidosis. *Lancet* **1995**, *345*, 767–772.
30. Wang, P.; Yi, T.; Xie, H.; Shen, F. a Novel Method for Diabetes Diagnosis Based on Electronic Nose. *Biosens. Bioelectron.* **1997**, *12*, 1031–1036.

31. Yu, J. B.; Byun, H.-G.; So, M.-S.; Huh, J.-S. Analysis of Diabetic Patient'S Breath with Conducting Polymer Sensor Array. *Sens. Actuators, B* **2005**, *B108*, 305–308.
32. Scislowski, P. W.; Pickard, K. The Regulation of Transaminative Flux of Methionine in Rat Liver Mitochondria. *Arch. Biochem. Biophys.* **1994**, *314*, 412–416.
33. Chen, S.; Zieve, L.; Mahadevan, V. Mercaptans and Dimethyl Sulfide in the Breath of Patients with Cirrhosis of the Liver. Effect of Feeding Methionine. *Lab Clin. Med.* **1970**, *75*, 628–635.
34. Tangerman, A.; Meuwese-Arends, M. T.; van Tongeren, J. H. New Methods for the Release of Volatile Sulfur Compounds from Human Serum: Its Determination by Tenax Trapping and Gas Chromatography and Its Application in Liver Diseases. *Lab Clin. Med.* **1985**, *106*, 175–182.
35. Smith, J. L.; Wishnok, J. S.; Deen, W. M. Metabolism and Excretion of Methylamines in Rats. *Toxicol. Appl. Pharmacol.* **1994**, *125*, 296–308.
36. Niwa, T.; Emoto, Y.; Maeda, K.; Uehara, Y.; Yamada, N.; Shibata, M. Oral Sorbent Suppresses Accumulation of Albumin-Bound Indoxyl Sulphate in Serum of Haemodialysis Patients. *Nephrol. Dial. Transplant* **1991**, *6*, 105–109.
37. Tamm, A.; Siigur, U.; Mikelsaar, M.; Vija, M. O. Output of Bacterial Metabolites As a Diagnostic Means. *Food* **1987**, *31*, 485–492.
38. Wardle, E. N.; Wilkinson, K. Free Phenols in Chronic Renal Failure. *Clin. Nephrol.* **1976**, *6*, 361–364.
39. Pirondini, L.; Dalcanale, E. Molecular Recognition at the Gas-Solid Interface: A Powerful Tool for Chemical Sensing. *Chem. Soc. Rev* **2007**, *36*, 695–706.
40. Reinhoudt, D. N. Molecular Recognition Applied to Sensors. *Sens. Actuators, B* **1995**, *B24*, 33–35.
41. Roeck, F.; Barsan, N.; Weimar, U. Electronic Nose: Current Status and Future Trends. *Chem. Rev.* **2008**, *108*, 705–725.
42. Albert, K.; Lewis, N. S.; Schauer, C. L.; Sotzing, G. A.; Stitzel, S. E.; Vaid, T. P.; Walt, D. R. Cross-Reactive Chemical Sensor Arrays. *Chem. Rev.* **2000**, *100*, 2595–2626.
43. Wold, S.; Esbensen, K.; Geladi, P. Principal Component Analysis. *Chemomet. Intel. Lab. Sys.* **1987**, *2*, 37–52.
44. Franke, R.; Gruska, A. Multivariate Data Analysis of Chemical and Biological Data. Principal Component and Factor Analysis. *Meth. Princ. Med. Chem.* **1995**, *2*, 113–163.
45. Li, J.; Lu, Y.; Ye, Q.; Cinke, M.; Han, J.; Meyyappan, M. Carbon Nanotube Sensors for Gas and Organic Vapor Detection. *Nano Lett.* **2003**, *3*, 929–933.
46. Byon, H. R.; Choi, H. C. Network Single-Walled Carbon Nanotube-Field Effect Transistors (SWNT-FETs) with Increased Schottky Contact Area for Highly Sensitive Biosensor Applications. *J. Am. Chem. Soc.* **2006**, *128*, 2188–2189.
47. Park, H.; Zhao, J.; Lu, J. P. Distinct Properties of Single-Wall Carbon Nanotubes with Monovalent Sidewall Additions. *Nanotechnology* **2005**, *16*, 635–638.
48. As indicated in the text, VOC-1 and VOC-4 appear in both healthy and CRF states but at different compositions. Therefore, using these two VOCs at the same concentration levels determined by GC-MS for healthy rates could serve as a simulative mixture for healthy states. Similarly, VOC-1 and VOC-5 appear in both healthy and CRF states but at different compositions. Therefore, using these two VOCs at the same concentration levels determined by GC-MS for real CRF rates, together with VOC-27 and VOC-29, which appear in CRF states only, could serve as a simulative mixture for CRF states.
49. Cao, W.; Duan, Y. Current Status of Methods and Techniques for Breath Analysis. *Crit. Rev. Anal. Chem.* **2007**, *37*, 3–13.
50. Lee, Y.; Kim, J. Simultaneous Electrochemical Detection of Nitric Oxide and Carbon Monoxide Generated from Mouse Kidney Organ Tissues. *Anal. Chem.* **2007**, *79*, 7669–7675.
51. Toda, K.; Li, J.; Dasgupta, P. K. Measurement of Ammonia in Human Breath with a Liquid-Film Conductivity Sensor. *Anal. Chem.* **2006**, *78*, 7284–7291.
52. Gaurava, K. A.; Malika, A. K.; Tewary, D. K.; Singh, B. a Review on Development of Solid Phase Microextraction Fibers by Sol-Gel Methods and Their Applications. *Anal. Chim. Acta* **2008**, *610*, 1–14.